SURFACE PROCESSES OF THE GREENLAND ICE SHEET UNDER A WARMING CLIMATE

Konrad Steffen, Thomas Phillips, and Kevin Sampson

University of Colorado at Boulder
Cooperative Institute for Research in Environmental Sciences
Campus Box 216, Boulder CO 80309

NASA Grant NNX08AT85G

Progress Report
to
National Aeronautics and Space Administration

May 2009

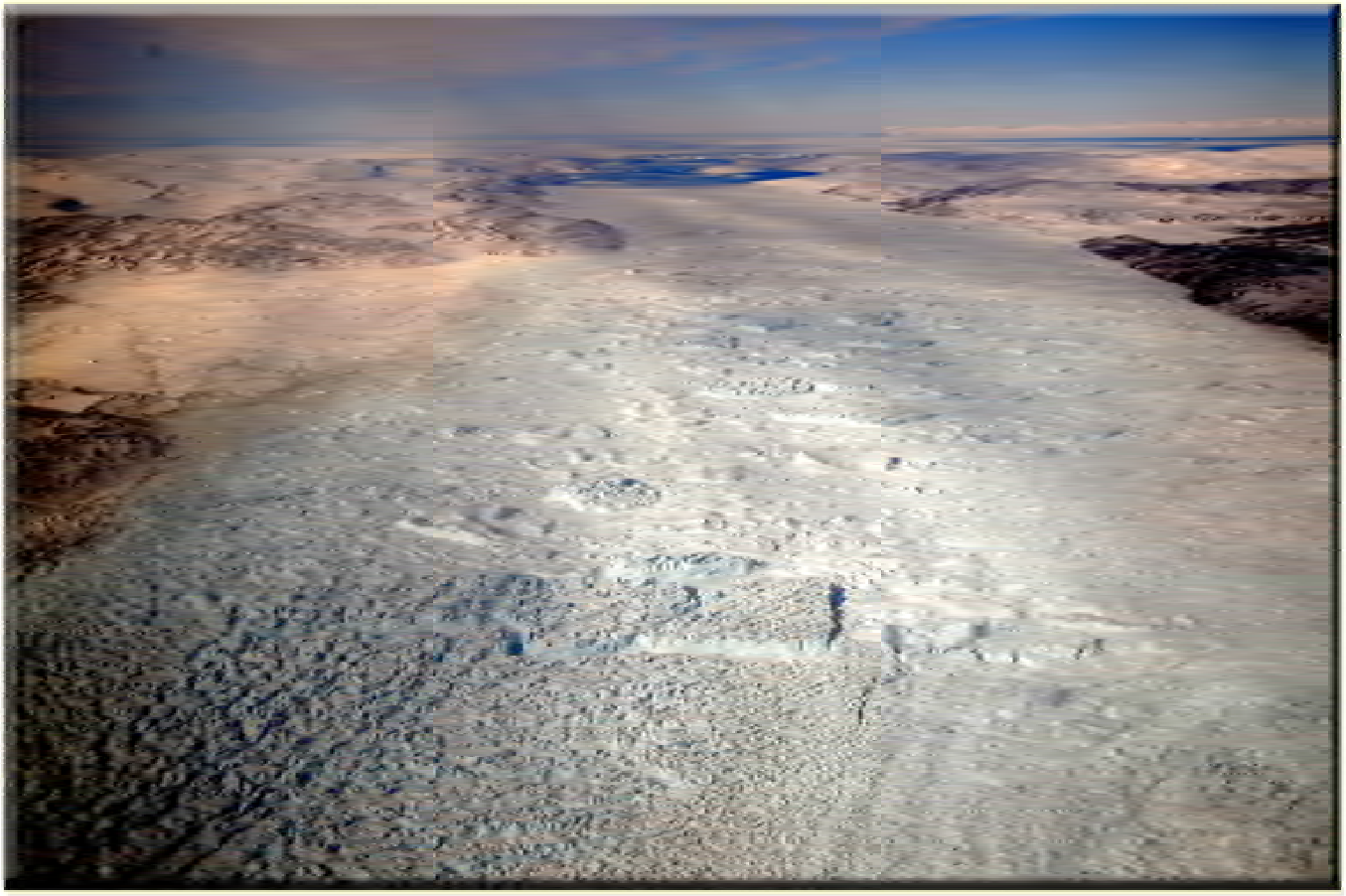

JAKOBSHAVN ISBRAE FLOATING ICE TONGUE, APRIL 28, 2009

Table of Content

1. Introduction

The Arctic climate has experienced some major changes in the past three decades. Natural climate variability is organized into spatial patterns of high and low pressure regions, the Arctic Oscillation, and the North Pacific patterns. The patterns of surface temperature anomalies when the AO are in their positive extreme are shown in Figure 1.1. When either of the patterns is in its positive extreme, the pattern contributes to an overall Arctic warm period. The North Pacific Pattern dominated the time period from 1977-1988 with above average temperatures in Greenland, followed by the dominate pattern of the Arctic Oscillation with below average temperatures for Greenland (Fig. 1.1). In recent years (2000–2005), however, the pattern of warm temperature anomalies is circumpolar in distribution and different from either of the two major 20th century climate patterns.

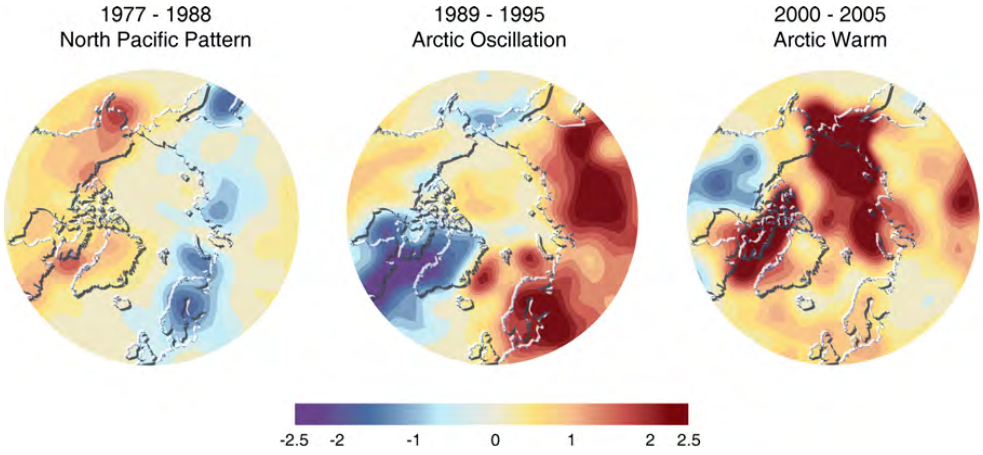

Figure 1.1: The three dominant pressure pattern for the Arctic during the past three decades resulting in a warm phase during 1977-1988, a cold phase during 1989-1995, and a warm phase during 2000-2005 for the Greenland ice sheet. The temperature scale is given in degrees Celsius.

The annual mean air temperature was found to be 2 ºC warmer for the central part of Greenland for the time period 1995–1999, as compared to *the* standard decade 1951–1960 [*Steffen and Box*, 2001]. Also, a notable increasing trend of 4.5% per year in melt area has been observed between the years 1979 and 1991, which came to an abrupt halt in 1992 after the eruption of Mount Pinatubo [*Abdalati and Steffen*, 1997]. The melt area is further increased with a periodicity of 3-4 years [*Abdalati and Steffen*, 2001]. The melt regions of the Greenland ice sheet have increased approximately 16% from 1979 to 2002 [*Steffen et al*., 2004] based on passive microwave satellite data. With the increased melt in the percolation region, the snow and firn layers have to increase in density due to the percolation and refreezing of melt water, hence reducing the surface height by near-surface densification.

In light of possible future sea level rise, a pressing need exists for precise knowledge of the mass balance of large ice sheets like Antarctica and Greenland. The deposition and accumulation of water as snow on the ice sheet are key components of mass balance. Changes of ice sheet thickness with time have been inferred from aircraft [*Krabill et al.*, 2000; *Thomas et al.*, 2003] and satellite data [*Zwally et al.*, 1998; *Davis et al.*, 1998]. Although little is known about Greenland's contribution to sea level rise during the past 50 years, observations from satellites and aircraft since 1990 show substantial ice loss from Greenland that has doubled in the last decade, both from increased runoff and from acceleration of glaciers draining the south of the ice sheet during a period of sustained local warming.

Ice locked within the Greenland ice sheet has long been considered comparatively immune to change, protected by the extreme cold of the Polar Regions. Most model results suggested that climate warming would result primarily in increased melting from coastal regions and an overall increase in snowfall, with net 21st century effects probably a small mass loss from Greenland and a small gain in Antarctica, and little combined impact on sea level. Observations generally confirmed this view, although Greenland measurements during the 1990s [*Krabill et al*., 2000; *Abdalati et al*., 2001] began to suggest that there might also be a component from ice-dynamical responses, with very rapid thinning on several outlet glaciers. Such responses had not been seen in prevailing models of glacier motion, primarily determined by ice temperature and basal and lateral drag, coupled with the enormous thermal inertia of a large glacier.

Increasingly, measurements in Greenland show rapid changes in the behavior of large outlet glaciers. Observations reveal glacier acceleration and this is happening along both the west and east coasts of Greenland [*Joughin et al., 2004; Howat et al., 2005; Rignot and Kanagaratnam*, 2006]. Such dynamic responses have yet to be fully explained, and are consequently not included in predictive models, nor is the forcing thought responsible for initiating them. Some of these processes are well summarized in the recent publication by the National Geographic Magazine "*The Big Thaw*" (Fig. 1.2), depicting some important surface processes on the Jakobshavn Isbrea.

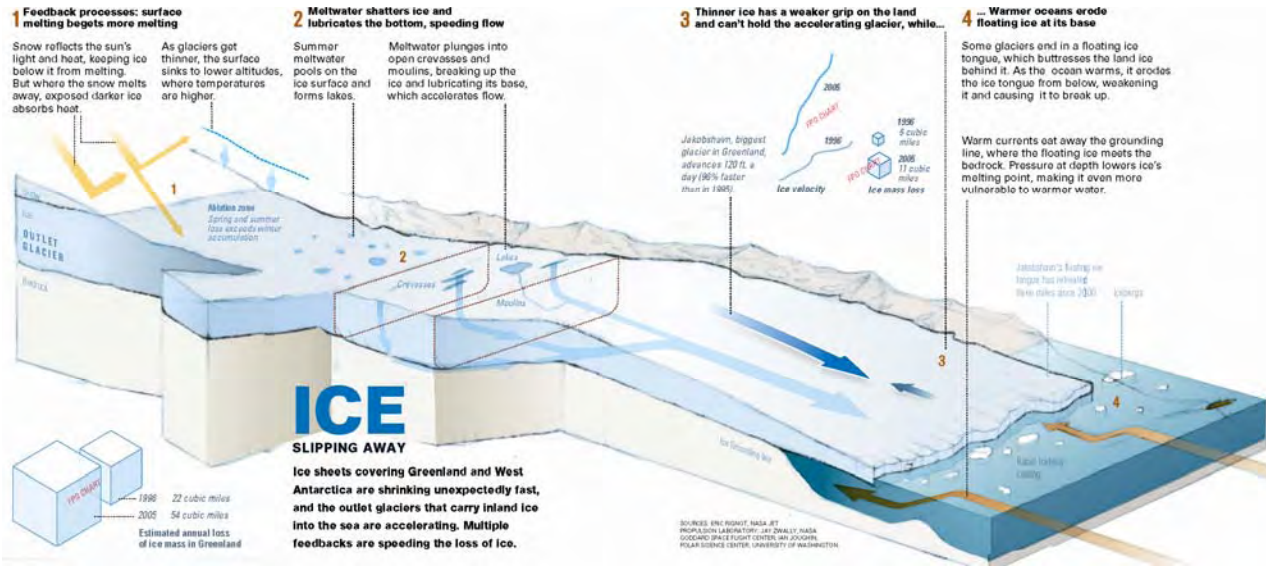

Figure 1.2: Schematic figure of an outlet glacier (Jakobshavn Isbrae) in Greenland showing the main surface processes.

The current mass loss of the Greenland ice sheet has the potential to become the dominate cryospheric contributor to sea level rise if the ablation region and outlet glaciers continue to lose mass at the current increasing rate. Surface processes that lead to the dynamic response of the ice under a warming climate need to be studied and monitored. Hence, long-term monitoring of meteorological and glaciological parameters is critical for the understanding of the surface processes, the forcings thereof, and model verification.

2. GC-Net Upgrade

The main objective for the 2009 field season is to upgrade the GC-Net with additional instruments and to ensure a timely and reliable hourly transmission of all the meteorological parameters via satellite link. Further, all the data will be made available instantaneously to the World Meteorological Organization (WMO). All stations would be registered as WMO stations, with a data feed to the US and European weather forecasting centers (NCEP and ECMWF). This would improve not only the weather forecast in high latitudes, but also provide crucial climate information of the Greenland ice sheet to monitor the current warming, the increase in surface melt, and the surface mass balance.

The data loggers in use are outdated and spare parts are no longer available. The new data loggers will allow higher temporal resolution (10 min mean) and they will conform to the new GOES satellite transmitter, installed north of 70 degrees N. Further, we will install new ventilated air temperature sensors, a new instrument to measure the surface temperature (IR sensor), new radiation sensors that measure net shortwave and net long-wave radiation, a GPS unit to track the ice motion at each GC-Net station.

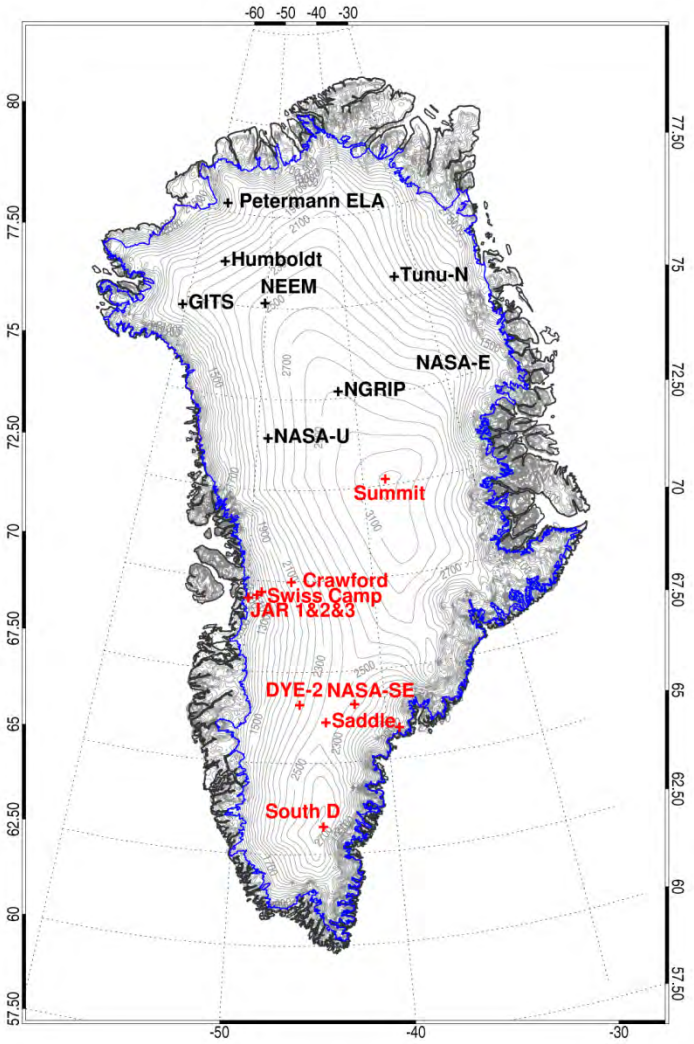

Fig. 2.1: Greenland Climate Network (GC-Net): Stations south of 70º N are using the geostationary GOES-W satellite (red color) for data transmission, whereas station north of 70º N (black color) using ARGOS polar orbiting satellites. NEEM in northwest Greenland is in support of the deep-ice core project and will be removed after the completion of the drilling project.

3. Results

3.1 Temperature Climatology at Swiss Camp: 1991-2008

The mean annual air temperature at Swiss Camp is -12.3° C (1991-2007), with the coldest monthly temperature in February (-32° C) and the warmest monthly temperature in July (Fig. 3.1). Summer months with above freezing occurred in 1995, and from 1997– present.

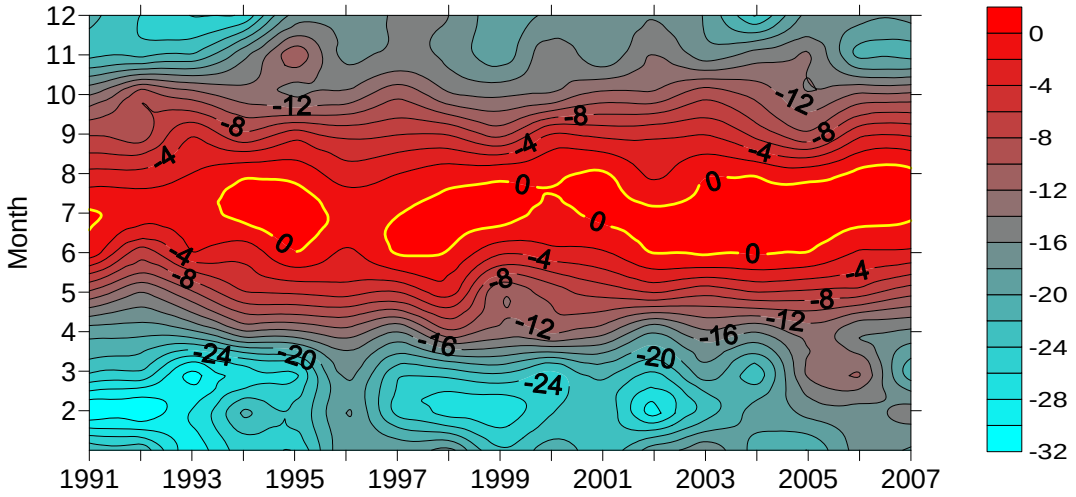

Figure 3.1: Interannual variability of monthly mean air temperatures (1991 – 2007) at the Swiss Camp, located at the equilibrium line altitude on the western slope of the Greenland ice sheet.

The mean annual temperature has increased by 4.3 ºC using a linear regression model as shown in Figure 3.2. The minimum temperature in 1992 was the result of the aerosol loading caused by the Mt. Pinatubo eruption. The linear regressing model at 95% confidence shows that the Pinatubo cooling and also the subsequent warming from the mid 90's were outside the 95% level of confidence. The warming that occurred since 2000 to present shows approximately the same trend then the 18-year time series. The warmest mean annual temperature was recorded with -9.9º C in 2008.

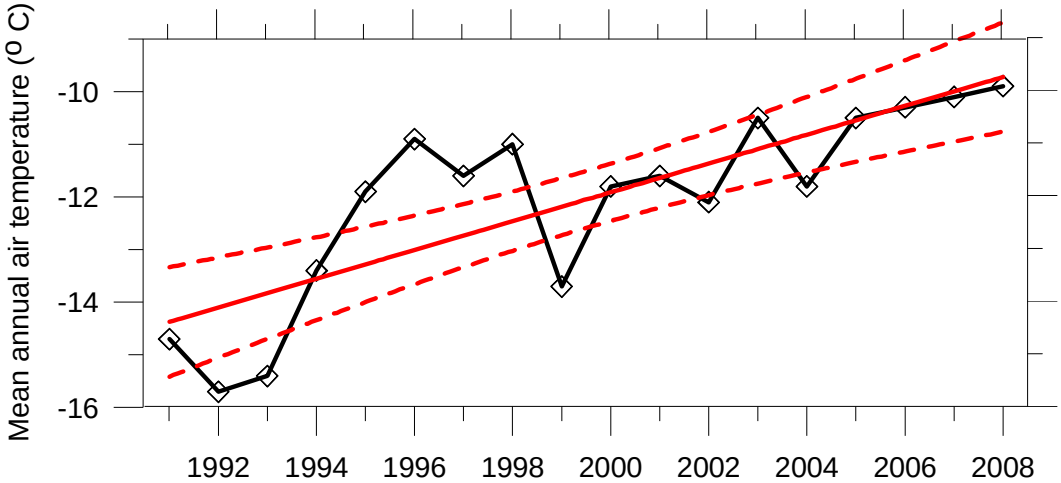

Figure 3.2: Swiss Camp mean annual temperature 1991 – 2008 (black line) with a linear regression model (red line) and 95% confidence levels (dashed red lines).

The statistical analysis of the Swiss Camp air temperature record reveals large interannual variability in all seasons with increasing temperatures throughout the recording period. The mean spring temperature increased from -17.5º C to -12.5º C, and fall temperature increased from -12.7º C to -11.0º C between 1991 and 2008, using a linear model. The winter temperature showed the largest increase of 6.3º C, whereas summer temperatures increased 2.3º C during the 16 years (1991 – 2008). The climate record at Swiss Camp shows a clear warming trend that started around 1995, consistent with the Arctic warming discussed in Fig. 1.1.

3.2 Radiation Climatology at Swiss Camp: 1993-2008

Radiation has been monitored continuously at Swiss Camp since 1993. The time series of mean monthly net radiation values is shown in Figure 3.3 (1993 – 2007). The largest monthly mean net radiation is found in summer 1995 (> 40 W m^{-2}), coincident with air temperatures above freezing, indicating a strong albedo-feedback mechanism at the ELA. Most of the annual snow cover melted and the bare ice surface was exposed, reducing the monthly albedo value to 0.6 (Fig.3.4).

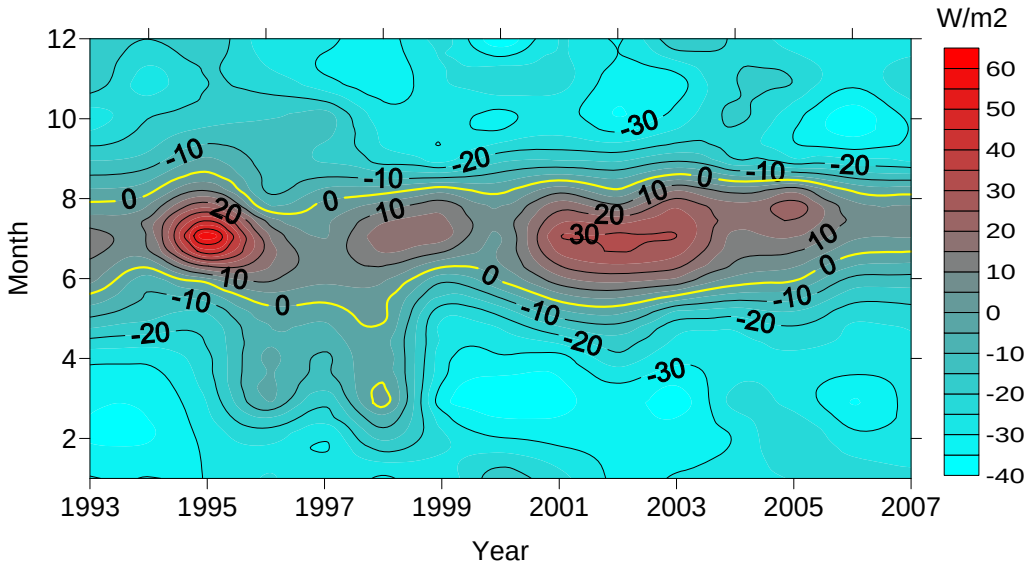

Figure 3.3: Interannual variability of monthly net radiation at the Swiss Camp (1993-2007).

It is worth discussing the three anomalous periods 1995, 1998, and 2001-2006 (Fig. 3.3). The summer season is characterized by a positive net radiation flux, which is indicative of the length of the melting High net radiation values can either be the result of low albedo values (i.e., 2003-2006, Fig. 3.4), reduced cloudiness (increase in insolation), or increase in atmospheric temperatures (increase in long-wave radiation). The mean summer net radiation has been higher during the new millennium (30 W m^{-2}) compared to the previous decade, with the exception of record high values in 1995, as a result of increased atmospheric temperatures leading to increase in surface melt (albedo reduction).

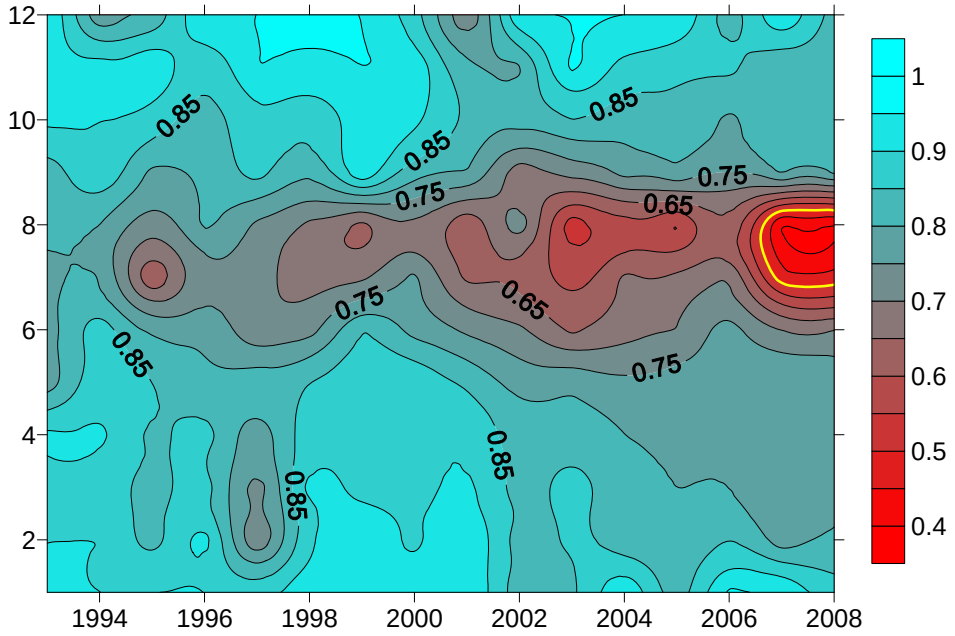

Figure 3.4: Interannual variability of monthly mean albedo at the Swiss Camp (1993 – 2008).

3.3 Accumulation and Ablation variability at Swiss Camp: 1990 – 2008

Interannual variability of snow accumulation varies between 7 and 70 cm water equivalent (w.e.), whereas the snow and ice ablation varies between 0 and 1.5 m (w.e.) for the time period 1990-2006. The mean net surface mass balance hovered around zero in the 90's with large deviations from the mean (Fig. 3.5), and a net mass loss is apparent starting in 2001 to present. The equilibrium line altitude (ELA) is no longer located at Swiss Camp (1100 m elevation) with a net surface loss of 1.75 m, and moved tent's of kilometers inland.

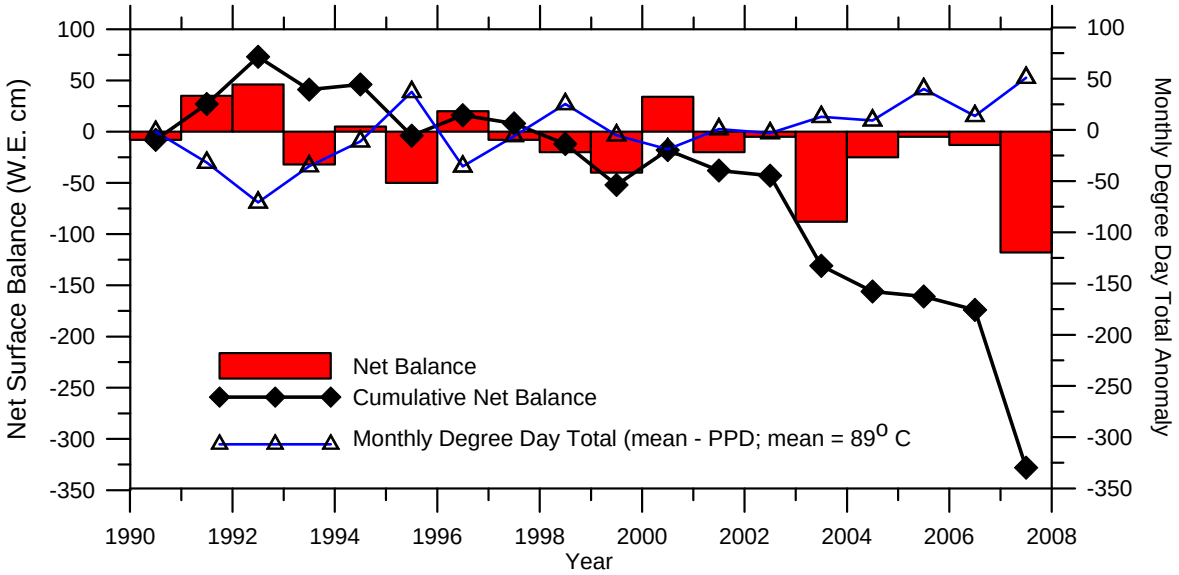

Figure 3.5: Net surface mass balance for the Swiss Camp location (red bars) total degree day totals normalized by the mean over the time period 1991-2008, and cumulative net balance (thick black line).

3.4 Firn Layer Climatology and Firn Compaction

Measurements of temperature and other climate variables for the Greenland ice sheet are continuously recorded by the Greenland Climate Network (GC-Net) surface meteorological stations. All GC-Net stations are equipped with a string of thermocouple temperature sensors to provide a record of the firn temperature profile as well as surface temperature and snow height change (*dH/dt*) sensors. Thermocouple temperature measurements have a relative accuracy of 0.1 ºC. A subset of six automatic weather stations is chosen that exhibits good spatial and temporal coverage of the extensive, high elevation (>2000m) accumulation regions of the interior of the ice sheet. The procedure to remove simultaneous temperature variations (STVs) in the thermocouples follows a newly developed, physically based data cleaning technique by *Cathles et al.* (2007). This method allows more physical process and parameter information to be extracted from the existing firn temperature data. To account for densification in the firn, and thus movement of the sensors relative to one another, a temperature-dependent model of firn densification is used which reproduces the strong seasonal signal in the densification rate of the upper firn. Further, the in situ time series of constant-depth temperatures at various levels are compared with modeled temperatures to validate the use of GC-Net data to estimate heat transfer into the snowpack.

We focus on data gathered by automatic weather stations (AWSs), distributed across the ice sheet at various locations and altitudes as part of the Greenland Climate Network (GC-Net; *Steffen et al.,* 1996). The stations were established in 1995 with the intention of exploring the climatology of the Greenland ice sheet (*Steffen and Box,* 2001). Only Stations from the GC-Net were used for this analysis of atmospheric and englacial temperatures due to their distributed spatial coverage, uniform construction, and uniform sensor configuration. The data is collected in a solid-state data logger, and transmitted via satellite to GC-Net researchers. Stations are also visited in regular intervals for maintenance and on-site data acquisition.

The assumption is made that areas which the XPGR method (*Abdalati and Steffen* 1995; 1997; 2001) does not indicate as exhibiting annual melt are in the dry snow zone and experience no melting and low melt intensity during the warm seasons. The AWS sites chosen are Humboldt Gl., Summit, Tunu-N, South Dome, NASA-E, and NGRIP, with site specific information listed in Table 3.1. Though South Dome occasionally experiences melt at the surface, the inclusion of this station is important for the representation of the southern GIS in this analysis.

Each GC-Net site is equipped with a string of thermocouples to monitor heat flux in the shallow firn layer near the station. This dataset was originally installed for monitoring the conductive heat flux that describes energy dissipation in the snowpack, and in particular for resolving heat input from latent heat release of refreezing meltwater (*Steffen et al.,* 1996; *Steffen and Box,* 2001). In addition to these applications, trends in firn and SAT can be assessed using this dataset. The instruments used are described in Table 3.1.

Data from 12 shallow firn cores (14 - 20 m) and one deep (~150 m) firn core from the regions around two GC-Net AWS stations were also used in this investigation. Six firn cores were retrieved from the Humboldt Gl. region in northwest Greenland (Humboldt Gl., 78.5266º N, 56.8305º W, 1995m) during the spring of 1995 (*Steffen et al.,* 1997). Two cores were taken in close proximity to the Humboldt Gl. AWS, within 5 m of each other, and four were taken at a distance of 25 km to the north, south, east, and west. The Humboldt firn core dataset contains 291 depth-density measurements ranging from 0.68 - 146.35 m depth. Depth-density data is used from seven additional ~15 m firn cores that were taken during the same field season in the Tunu region of northeast Greenland (Tunu-N, 78.0168º N, 33.9939º W, 2020m). The dataset at Tunu features 105 depth-density measurements, taken at depths from 0 - 14.04 m. The cores were drilled within a 100 km^2

area, at 25 and 50 km distance north, east, and west of Tunu-N AWS. The depth-density measurements from these cores were used to validate firn compaction model results.

Table 3.1. Location, altitude, and inception date of GC-Net permanent AWS stations used in this study.

ID#	Name	Latitude	Longitude	Elev.[m]	Start Date
5	Humboldt Gl.	78.5266	56.8305	1995	1995.47
6	Summit	72.5794	38.5042	3208	1996.37
7	Tunu-N	78.0168	33.9939	2020	1996.38
11	South Dome	63.1489	44.8167	2922	1997.31
12	NASA-E	75.0000	29.9997	2631	1997.34
14	NGRIP	75.0998	42.3326	2950	1997.52

Variability in the density profile of an ice sheet is due to changes in temperature, accumulation rate, and the density of recently deposited snow near the surface of the ice sheet (*Arthern and Wingham,* 1998). Thus, the dH/dt at time *t* is the sum of accumulation $A(t)/\rho_0$, firn densification $V_{fc}(0,t)$, advection and thinning of ice V_{ice}, and surface ablation $B(t)$, such that

$$\frac{dH(t)}{dt} = \frac{A(t)}{\rho_0} - V_{fc}(0,t) - V_{ice} - B(t).$$

This equation is identical to Equation 1 in *Zwally and Li* (2002). The term V_{ice} is neglected here because changes in vertical velocity of ice and crustal motion underneath the ice sheet are not observed by the GC-Net acoustic surface height sensor. Though ablation $B(t)$ is incorporated into the dH/dt signal, the term may be neglected in dry zones of the GIS (*Zwally and Li,* 2002). Snow densification and accumulation are incorporated into the dH/dt signal at each time-step, because sub-surface densification will act to lower the surface recorded by the sensor. Thus, Equation 3.1.1 is simplified in this analysis to become

$$\frac{dH(t)}{dt} = \frac{A(t)}{\rho_0} - V_{fc}(0,t).$$

Differential firn densification with depth can act to push sensors together and disrupt the even-spacing of the original sensor placement. For these reasons it is necessary to attempt to model densification of snow layers between sensors in the shallow firn to achieve a correct depth-density profile as well as a correct accumulation time-series.

A model intercomparison was created to assess the suitability of different firn compaction models. The models tested were *Schytt* (1958), *Kojima* (1967), *Herron and Langway* (1980), and *Zwally and Li* (2002). The best model for simulating firn compaction based on available GC-Net data is that of *Zwally and Li* (2002). The model allows for the input of surface temperature and dH/dt at each time step, allowing for seasonal temperature variations to cause differential compaction with time. Figure 3.6 shows the model reconstruction of *in-situ* firn core data taken from the Humboldt and Tunu regions in northern Greenland.

The model is initialized with a depth-density profile that closely resembles *in-situ* firn core data, and drives sub-surface temperature with the GC-Net recorded surface temperature. The original placement of subsurface thermocouple temperature sensors is input and the densification between

layers and depth of each sensor relative to the surface is calculated. Figure 3.7 illustrates the relative-depth trajectory of temperature sensors based on firn densification calculated with the *Zwally and Li* (2002) compaction model.

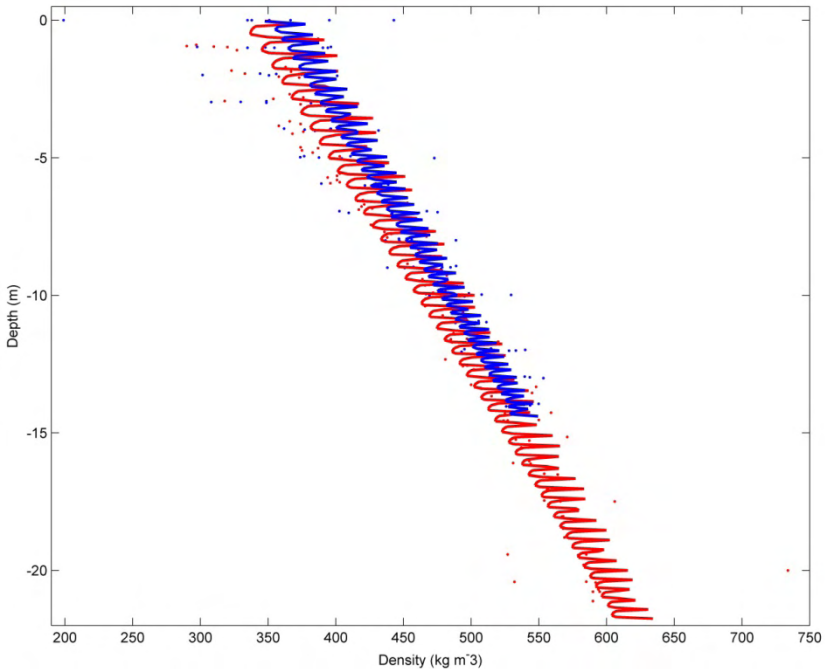

Figure 3.6: Best fit curves of ρ(z) based on Zwally and Li (2002) for Humboldt (red line) and Tunu (blue line). Dots represent in-situ firn core data.

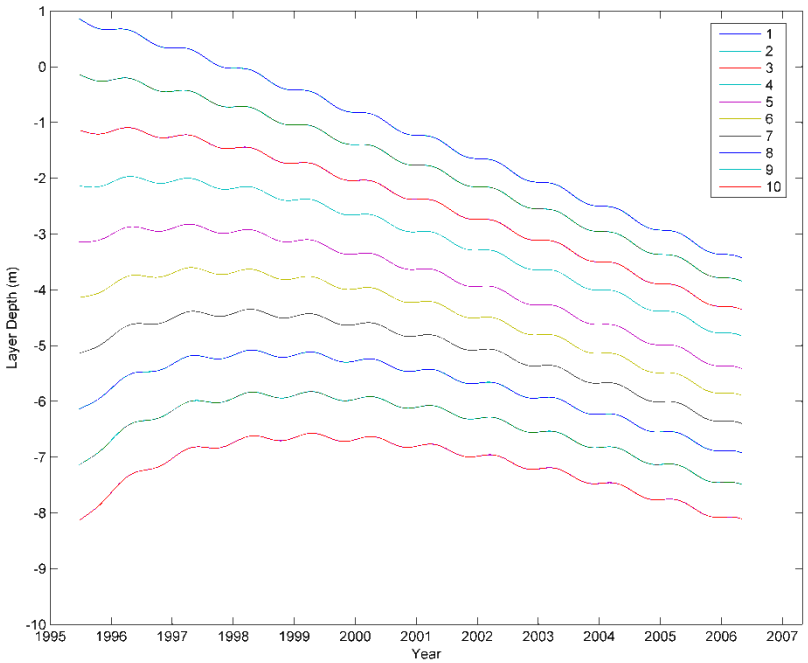

Figure 3.7: Depth of each sensor in the GC-Net thermocouple string at Humboldt Gl. AWS relative to the surface. Densification is calculated using Zwally and Li (2002).

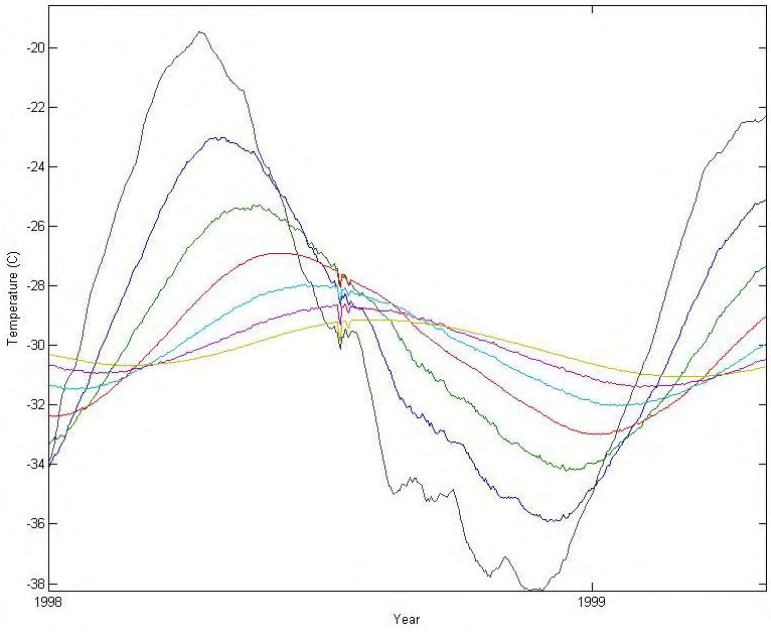

Figure 3.8: Measured temperature cycles at 10 depths at NASA-E AWS after STV correction.

3.5 Firn Temperature

In order to make the dataset more suitable for analysis, the analysis of temperature data must compensate for variations in depth using the initial depth at the time of sensor deployment, and adjusting for the surface height change (dh/dt) that is recorded by the surface height gauges. The problem was noted by Schytt (1960) though not corrected.

The depth-correction for the thermocouple sensors is based on the *Zwally and Li* (2002) firn densification model. The model is forced with GC-Net surface temperature, and the sensor depths are initialized based on the depth of sensors at station inception. The model is run forward in time as the depth of each sensor relative to the surface is calculated based on the rate of accumulation and densification. The correct depth-temperature profile is then calculated by linear interpolation between sensors. The sensors begin at 1 m intervals but are pushed together as the snow between them compacts. Thus, the error in interpolation is never more than ½ of the difference of two adjacent sensor temperature values. Because temperature varies little with depth, the error is minimal.

Surface temperature from GC-Net stations for each AWS site in this study are listed in Tables 3.2 and 3.2. Firn temperature time-series are currently being conducted by GC-Net researchers and results will be available shortly.

Table 3.2 GC-Net Surface Temperature measurements

Site	Maximum T	Minimum T	Amplitude*
Humboldt Gl.	June 10	December 9	32.6° C
Summit	July 17	January 15	29.4° C
Tunu-N	July 18	January 16	33.4° C
South Dome	June 10	December 9	21.9° C
NASA-E	July 17	January 15	29.8° C
NGRIP	July 19	January 17	32.1° C

* Peak-to-peak amplitude

Table 3.3 GC-Net Surface Temperature statistics

Site	Maximum T	Minimum T	Mean	Trend
Humboldt Gl.	4.9° C	-61.4° C	-26.1° C	0.09° C a^{-1}
Summit	-0.5° C	-59.4° C	-29.6° C	-0.07° C a^{-1}
Tunu-N	3.7° C	-59.0° C	-27.7° C	0.11° C a^{-1}
South Dome	5.2° C	-53.2° C	-19.3° C	0.02° C a^{-1}
NASA-E	4.6° C	-57.7° C	-27.9° C	0.02° C a^{-1}
NGRIP	2.5° C	-68.1° C	-28.4° C	0.13° C a^{-1}

* Italics indicates significant trend ($p < .01$)

3.5 Cross Correlation of Ice Temperature with Snow Height

The cross correlation of the ice temperatures in respect to the snow height was performed in SPSS. This was done for the simple reason that MatLab failed to provide results. The lag time was set to 1 month.

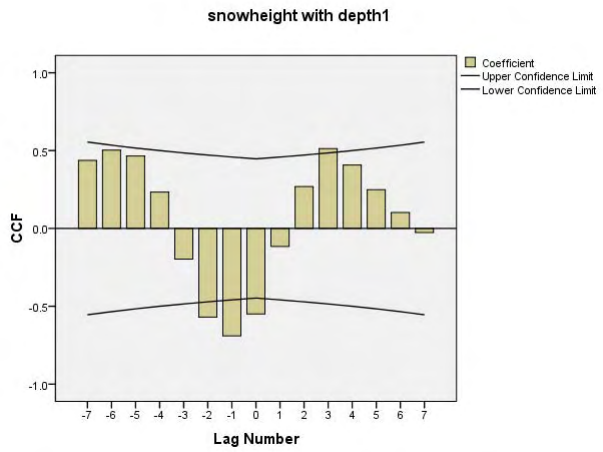

Figure 3.9: Cross correlation of snow height for 2001/02 with the ice temperature at 1 meter depth. The lag size is set to 1 month. The 95% confidence intervals are shown in black. The y-axis displays the correlation coefficient.

For temperatures at 1 meter depth there is a positive correlation at 2 months lag and a strongly negative correlation for 2 through the current month (compare Figure 3.9). This means that if the snow cover decreases, the ice temperature increases. This is strongly the case especially for the summer months. The positive two month lag may be due to the winter where a thicker snow cover results in a higher ice temperature.

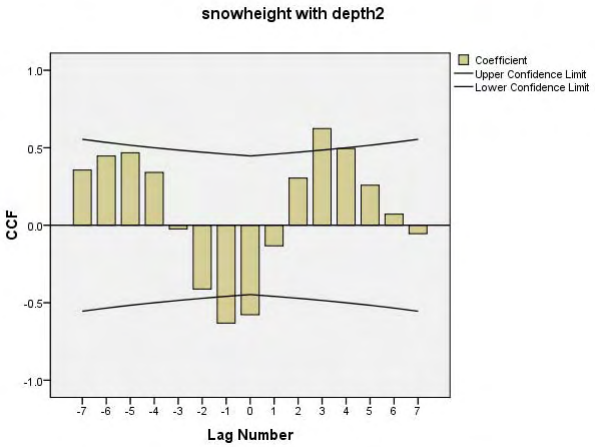

Figure 3.10: Cross correlation of snow height for 2001/02 with the ice temperature at 2 meter depth. The lag size is set to 1 month. The 95% confidence intervals are shown in black. The y-axis displays the correlation coefficient.

The results for the cross correlation of the snow height with the ice temperature at 2 meters depth can be interpreted in a similar way as for 1 meter depth. For temperatures at 2 meter depth there is a positive correlation at 2 months lag, and a strongly negative correlation for -2 through the current month (Figure 3.10). This means that if the snow cover decreases, the ice temperature increases. This is strongly the case especially for the summer months. The positive two month lag may be due to the winter where a thicker snow cover results in a higher ice temperature. In addition there is a positive correlation for 3 months lag which may indicate that it takes longer for the surface temperature to reach the depth. This would be as expected.

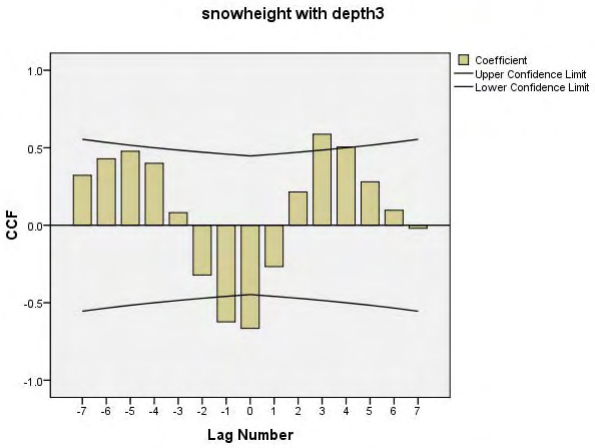

Figure 3.11: Cross correlation of snow height for 2001/02 with the ice temperature at 3 meter depth. The lag size is set to 1 month. The 95% confidence intervals are shown in black. The y-axis displays the correlation coefficient.

At three meters depth we see virtually the same result as for at 2 meters depth (Figure 3.11). The lag is getting longer though and the negative correlation for -2 months is not significant any more. This means that the summer ice free time does not have the same strong effect as for the previous depths.

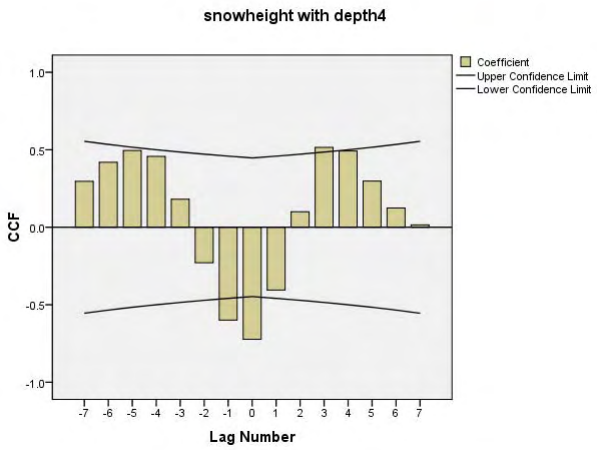

Figure 3.12: Ccross correlation of snow height for 2001/02 with the ice temperature at 4 meter depth. The lag size is set to 1 month. The 95% confidence intervals are shown in black. The y-axis displays the correlation coefficient.

In Figure 3.12 the cross correlation for the temperature at 4 meters depth is described. The correlation at the +3 month lag is becoming stronger than the equivalent at the +2 month lag. This indicates the conduction time from the surface increases as expected. The negative correlation is still strongly visible due to the summer months.

In Figure 3.13 there is no positive significant correlation anymore. There is still a strong negative correlation for the -1, 0 and +1 lag correlations. This means that when the snow cover is low, the ice temperature is high and vice versa. If you compare this to Figure 3.6 it becomes clear that this is the case not only for the upper 5 meters of depth but for the entire temperature profile. As a result no further cross correlation analysis was performed. It is interesting though that such a strong oscillation at the various depths is visible. No temperature trend could be detected but 20 months is probably too short. The standard deviation for each depth is listed in table 3.4.

Table 3.4: The standard deviation of the temperatures at each depth indicating the size of the amplitude.

Depth	1meter	2 meter	3 meter	4 meter	5 meter	6 meter	7 meter
Std dev	5.5 C	4.7 C	4.1 C	3.5 C	2.9 C	2.5 C	2.1 C

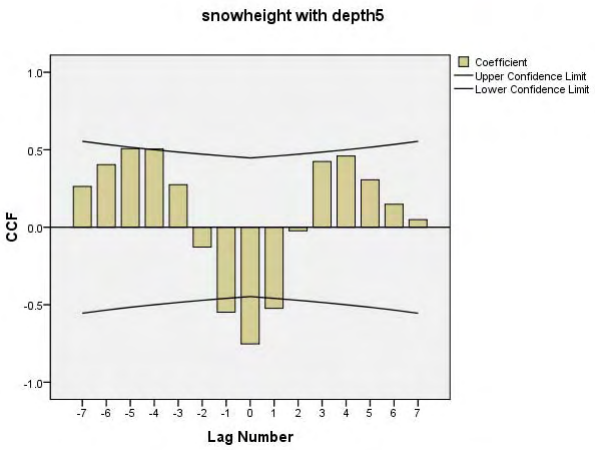

Figure 3.13: Cross correlation of snow height for 2001/02 with the ice temperature at 5 meter depth. The lag size is set to 1 month. The 95% confidence intervals are shown in black. The y-axis displays the correlation coefficient.

Table 3.5: The physical properties density (ρ), heat conductivity (k) and heat capacity ($\mathbf{c_p}$) for different snow and ice. The diffusivity term κ increases for lighter snow.

Material	Porosity $[\frac{\%}{100}]$	κ $[\frac{m^2}{s}]$	ρ $[m^3]$	k $[\frac{W}{mK}]$	c_p $[\frac{J}{kgK}]$
ice	0	1.14e-6	917.0	2.10	2000
snow	0.1	1.12e-6	825.3	1.80	1800
snow	0.2	1.30e-6	733.6	1.53	1600
snow	0.3	1.42e-6	641.9	1.28	1400
snow	0.4	1.58e-6	550.2	1.05	1200
snow	0.5	1.83e-6	458.5	0.84	1000
Snow (melt starts)	0.6	2.20e-6	366.8	0.65	800
Snow	0.7	2.82e-6	275.1	0.47	600
New snow	0.8	4.09e-6	183.4	0.30	400

In table 3.5 the diffusivity term κ for the different snow densities are compared to the diffusivity term for ice. Diffusivity is the product of heat conduction heat capacity as well as the density of the material:

$$\kappa = \frac{k}{c_p * \rho}$$

The interesting fact is that the lower the density of snow the higher the heat diffusivity term becomes. Snow has lower conduction as well as a lower heat capacity.

4. Proposed Field Activities and Research Objectives 2009

4.1 AWS Maintenance

The automatic weather station network will be maintained and upgraded. In the south, the Petermann ELA stations will be serviced as part of the NSF/NASA supported field activities. In the southern part of the ice sheet we will service the DYE-2, Saddle, NASA SE, Saddle, and S-Dome (Fig. 2.1), download the data and collect snow stratigraphy information.

Further, NASA-U, and Summit will be serviced in late May, and we will visit the new NEEM AWS to download the data and relocate the station to close to the new drilling camp. The profile JAR2, JAR1, CU/ETH, and Crawford 1 will be serviced while at the Swiss Camp.

The field season 2009 will concentrate to upgrade AWS's on the Greenland ice sheet with updated data loggers and some new instrumentation. Further, we will install new GPS unites for those AWS's that transmit via GOES satellite and need a very accurate time stamp. Several AWS's have melted out in the ablation region near Swiss Camp and need to be re-drilled.

4.2 GPS Network Maintenance

Our effort to monitor the ablation along a transect from the Swiss Camp to the ice margin will continue. We will service the GPS network in collaboration with Dr. Jay Zwally (NASA-GSFC) and will add two new GPS monitoring stations in the Jakobshavn region. We will continue to collect high-resolution surface topography data using Trimble Pathfinder differential GPS measurements along several transects in the lower ablation region. In addition, we will acquire a sequence Landsat TM satellite imagery during the onset of melt and melt period to monitor the spatial variation and extent of snow fields in the ablation region.

4.3 Ground Penetration Radar

We have collected a number of ground penetrating radar (GPR) profiles along the western slope of the ice sheet (Jakobshavn and Kangerlussuaq region) in previous field seasons (1999, 2000, 2003, and 2007). The analysis of this data set showed that the accumulation could vary up to 40% between the trough and the ridge of the undulation. The surface topography with scale length of several kilometers plays an important role for the spatial variability of accumulation, the mass transfer, and the surface energy balance. We will repeat some of these GPR measurements during the spring 2009 field season along the same profiles to verify the recent accumulation changes and high percolation events in that region. We also purchased a new MALA 10 KHz ground penetrating antenna to map the underside of the Greenland ice sheet below Swiss Camp towards the ice margin in view of our moulin modeling. We will try to assess the sub glacial conduit density and the occurrence frequency of moulin (relics) in spring 09.

5. Bibliography

Abdalati, W. and K. Steffen, Greenland ice sheet melt extent: 1979-1999, *J. Geophys. Res.*, 106(D24), 33,983-33,989, 2001.

Abdalati, W., and K. Steffen, The apparent affects of the Mt. Pinatubo eruption on the Greenland ice sheet melt extent, *Geophys. Res. Lett*., 24(14), 1795-1797, 1997.

Abdalati, W., and K. Steffen, Passive microwave-derived snow melt regions on the Greenland ice sheet, *Geophys. Res. Lett.*, 22, 787-790, 1995.

Abdalati, W., W. Krabill, E. Frederick, S. Manizade, C. Martin, J. Sonntag, R. Swift, R. Thomas, W. Wright and J. Yungel, 2001, Outlet glacier and margin elevation changes: Near-coastal thinning of the Greenland ice sheet. *J. Geophys. Res*., **106** (D24), 33729-33741, 2001.

Abdalati, W., and K. Steffen, Passive microwave derived snowmelt regions on the Greenland ice sheet. *Geophysical Research Letters* 22(7), 787-790, 2001.

Arthern, R. J., and D. J. Wingham, The natural fluctuations of firn densification and their effect on the geodetic determination of ice sheet mass balance. *Climatic Change* **40**, 605-624, 1998.

Cathles, L. Maclagan IV, L. M. Cathles III, and M. R. Albert, A physically based method for correcting temperature profile measurements made using thermocouples. *Journal of Glaciology* **53**(181), 298-304, 2007.

Davis, C.H., C.A. Kluever, and B.J. Haines, Elevation change of the southern Greenland ice sheet, *Science*, 279, 2086-2088, 1998.

Herron, M. M., and C. C. Langway, Jr., Firn densification: an empirical model. *Journal of Glaciology* **25**(93), 373-385, 1980.

Howat, I. M., I. Joughin, S. Tulaczyk, and S. Gogineni, Rapid retreat and acceleration of Helheim Glacier, east Greenland. *Geophys. Res. Lett*., **32** (L22502), 2005.

Joughin, I., W. Abdalati, M. Fahnestock: Large fluctuations in speed on Greenland's Jakobshavn Isbrae glacier. *Nature*, 432, 608-610, 2004.

Kojima, K., Physics of snow and ice. *Contribution* **799,** *Proceedings of the International Conference on Low Temperature Science, Sapporo, Japan,* 929-952, 1967.

Krabill, W. W. Abdalati, E. Frederick, S. Manizade, C. Martin, J. Sonntag, R. Swift, R. Thomas, W. Wright, and J. Yungel, Greenland ice sheet: high-elevation balance and peripheral thinning, *Science*, 2000.

Rignot, E. and P. Kanagaratnam, Changes in the Velocity Structure of the Greenland Ice Sheet. *Science*. 311: 986-990, 2006.

Schytt, V., The inner structure of the ice shelf at Maudheim as shown by core drilling. *Norwegian-British-Swedish Antarctic Expedition, 1949-52, Scientific Results* **4**, *Glaciology 2.* Norsk Polarinstitutt, Oslo, 115-151, 1958.

Steffen, K. and J. Box, Surface climatology of the Greenland ice sheet: Greenland Climate Network 1995-1999, *Journal of Geophysical Research* 106(D24), 33,951-33,964, 2001.

Steffen, K., S.V. Nghiem, R. Huff, and G. Neumann, The melt anomaly of 2002 on the Greenland Ice Sheet from active and passive microwave satellite observations, *Geophys. Res. Lett*., 31(20), L2040210.1029/2004GL020444, 2004.

Steffen, K., A. Nolin, J. White, Assessment of Variations in the Snow Accumulation Rate in Northern Greenland. Annual Progress Report to National Science Foundation. NSF/OPP 9423530, pp.14, 1997.

Steffen, K. J. Box, and W. Abdalati, Greenland Climate Network: GC-Net. *CRREL Report on Glaciers, Ice Sheets, and Volcanoes*, No. **96-27**, 98-103,l 1996.

Thomas, R.H., W. Abdalati, E. Frederick, W.B. Krabill, S. Manizade, and K. Steffen, Investigation of surface melting and dynamic thinning on Jakobshavn Isbrea, Greenland, *J. Glaciol*., 49(165), 231-239, 2003.

Zwally, H,J., A.C. Brenner, and J.P. DiMarzio, Comment: Growth of the southern Greenland ice sheet, *Science*, 281, 1251, 1998.